DNA relaxation dynamics as a probe for the intracellular environment

J. K. Fisher[a,1], M. Ballenger[b], E. T. O'Brien[b], J. Haase[c], R. Superfine[b], and K. Bloom[c]

Departments of [a]Biomedical Engineering, [b]Physics and Astronomy, [c]Biology, University of North Carolina, Chapel Hill, NC 27599

Investigations into the biophysical properties of single molecules traditionally involve well defined in vitro systems where parameters such as solvent viscosity and applied forces are known a priori. These systems provide means to develop models describing the polymers response to a variety of conditions, including the entropically driven relaxation of a stretched biopolymer upon release of the tension inducing force. While these techniques have proven instrumental for recent advancements in the fields of polymer physics and biophysics, how applicable they are to life inside the cell remains poorly understood. Here we report an investigation of in vivo stretched polymer relaxation dynamics using chromatin relaxation following the breakage of a dicentric chromosome subjected to microtubule-based spindle forces. Additionally, we have developed an in vitro system used to verify the conformations observed during the in vivo relaxation, including the predicted but previously unidentified taut conformation. These observations motivate our use of existing polymer models to determine both the in vivo viscosity as seen by the relaxing chromatin and the tension force applied by the microtubule-based spindle in vivo. As a result, the technique described herein may be used as a biophysical strategy to probe the intranuclear environment.

intranuclear viscosity | stem and flower

Single molecule analysis of fluorescently labeled DNA under tension has been used in a variety of investigations of polymer dynamics (1–6) in vitro. Traditionally these experiments have been performed using electrophoresis (7) or, more commonly, fluid flow to extend the polymer, with the dynamics of the polymer being investigated at either constant extension [corresponding to a fixed voltage or specific flow rate (2, 5, 8)] or after the flow is stopped (4, 9, 10). In the latter case, the elimination of the stretching force causes the chain to relax from its free end, allowing the relaxation dynamics to be observed. For a relaxing polymer chain, a number of different conformations may be observed as the constraint release propagates throughout the chain (Fig. 1). As a result, relaxation events may be broken up into multiple regimes, each corresponding to a different polymer conformation, with the expressions used to describe the length of the polymer over time yielding information about either polymer specific properties, such as the tension force applied immediately before recoil, or the viscosity of the surrounding environment.

While much is known about the mechanism of sister chromatid separation, surprisingly little is known about fundamental quantities such as the forces that are generated by microtubule-based spindles under physiologically relevant loading (i.e., what forces are generated during sister separation) and the intranuclear viscosity. A lack of noninvasive in vivo data collection techniques provided the impetus for developing alternative in vitro or in silico experiments, but very few opportunities to confirm that the assumptions made in these experiments, much less the results themselves, are accurate. As a direct consequence, data collected from an in vivo system will be beneficial because, in addition to determining fundamental cellular quantities, it will offer an opportunity to determine if an in vitro system accurately represents the in vivo environment and provide a means to determine if assumptions made in simulations (i.e., solvent type) are reasonable.

Polymer models derived by Brochard-Wyart (11) predict that a stretched DNA chain subject to a uniform tension force f will be in a taut regime if φ, where $\varphi = f l_{po}/k_B T$ (l_{po} the unperturbed persistence length, k_B Boltzmann's constant, and T the temperature) is greater than 1. This taut regime, typically experienced at tension forces well below 1 pN, corresponds to DNA extended beyond the linear (Hookean) region of the worm-like chain (WLC) model (12) and into a nonlinear regime where the tension force suppresses bending modes in the links of the polymer chain. Put differently, at this applied force, the length scale at which the chain conformation is randomized due to thermal forces (also known as the tension blob diameter) is shorter than the persistence length of the chain. As a result, the chain's conformation appears oriented at all length scales. In Fig. 1*A*, the expected physical conformations for the chain, relative to this threshold force, are illustrated (conceptual tension blobs shown in pink). Beyond this force threshold, the worm-like chains are stiff, but not completely rigid; the links may still fluctuate and bend*. It is the straightening of the bends that is responsible for extension in this regime. If the force is released at one end, the chain will retract, taking on the conformations shown in Fig. 1*B*. The chain will initially retract with a fast time constant τ_1, where τ_1 is given by $\tau_1 = L^2/D_0 \eta \varphi^{3/2}$. Here L is the length of the chain, and $D_o = 4 k_B T/k_v \eta l_{po}$, with $k_v = 1$. The relaxation of the taut chain is characterized by the uniform uptake of additional length by each segment of the chain, so that each segment of the chain appears similar; the chain is regaining the bends and fluctuations in the links that were lost during the stretch in the nonlinear regime. After time τ_1, the chain will relax from the rod-like or taut conformation to a new, independent conformation described by Brochard-Wyart as the "stem and flower" (13). In this regime, where $\varphi = f l_{po}/k_B T$ is less than 1, the flower describes a portion of the polymer at the leading end of the retracting molecule where the tension is significantly lower than that of the remaining portion, which is called the stem (Fig. 1). With time the flower consumes the stem, causing both the flower to grow and the stem to shrink according to $L \approx (kTt/\eta l_{po})^{1/2}$. Since in this conformation the polymer is completely described by the flower and stem portions of the chain, the previous expression may also be used to describe the total change in length of the DNA chain while in the stem and flower conformation.
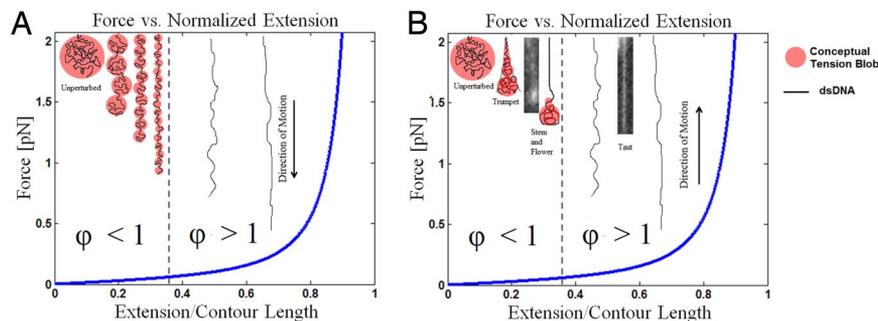

Fig. 1. Summary of the expected conformations for the polymer during extension and retraction with tension blob representation of the length scale at which thermal forces randomize the conformation of the polymer. (*A*) As the applied tension force increases during stretching, the length scale at which thermal forces randomize the orientation of the segments of the polymer decreases until it is smaller than the size of the Kuhn monomer (threshold indicated by the vertical dashed line). (*B*) As the polymer retracts, the taut conformation without tension blobs gives way to the stem and flower conformation where a tension blob forms at the retracting end and is visible in the form of a ''flower.'' Insert images from in vitro experiments showing a retracting polymer in the taut and stem and flower conformations are shown next to the illustrations of these conformations. This diagram assumes the retracting polymer will not be affected by boundaries. While combinations of these conformations are possible (i.e., portion of stem in stem and flower taking on trumpet conformation), we assume the majority of in vivo relaxation will fall into one of these general categories.

While the utility of such models for determining in vitro biophysical properties is clear, the experimental techniques necessary for similar investigations, as well as the applicability of these same models to in vivo biopolymer relaxation are not readily apparent. In this report, we describe a genetic approach to obtain relaxation events from stretched chromatin [the protein-DNA complex found inside a cell (14)], as well as the development of an in vitro system that has been used to verify data analysis techniques. In both cases, the use of these models is supported by correlating the fluorescent intensity of the retraction images with the general polymer shape expected by the models and by the application of a scaling analysis. The result of this work includes the first observation of the predicted relaxation of a taut (rod-like) polymer conformation (11), the observation of entropic relaxation of DNA in vivo, an in vivo measurement of the mesoscale intranuclear viscosity, and an estimate of the force applied by the microtubule-based spindle.

Results

Chromatin Relaxation In Vivo. Molecular motors acting within the mitotic spindle may be used as in vivo force applicators on a single strand of chromosomal DNA by tethering 1 strand to both spindle poles of the mitotic apparatus. This was accomplished through the use of conditionally functional dicentric chromosomes (14) as shown in Fig. 2 and described in greater detail in the *Materials and Methods* section. Briefly, a 10-kb lac operator (lacO) repeat was located nearly equidistant from both the endogenous and the integrated centromere and made visible by expression of lacI-GFP. In *sir2* mutant cells, activation of a

lacO-marked dicentric chromosome results in stretched lacO filaments that either persist until spindle collapse, or rupture, allowing visualization of the DNA as it recoils toward the spindle poles (Fig. 3). In the case of the latter, little hysteresis is seen; lacO filament stretching rates are very similar to the rate of recoil. Chromosome breakage is stochastic and was observed at random positions between the 2 spindle poles. The behavior of chromatin following DNA breakage exhibits a period of fast relaxation followed by a period of slower relaxation. Fluorescent images taken of the retracting biopolymer (Figs. 3*A* and 4*A*) show that within the first few frames of the relaxation event, the end-to-end length of the biopolymer shrinks by almost half. For the same period, the montage shown in Fig. 4*B* displays a constant intensity near the retracting end of the fiber. Capturing this spontaneous in vivo rupture event is indeed a rare occurrence (*n* = 3), but all instances of recoil in this system demonstrate the characteristics described herein.

DNA Relaxation In Vitro. Determining the conformation directly from the fluorescent images is difficult for in vivo data due to the complexity of the in vivo situation. The background signal

Fig. 2. Spindle attachments and dicentric chromosome breakage. (*A*) Attachment of both centromeres of a given sister chromatid to the same spindle pole. Decatenation of DNA strands allows sister chromatids to separate and segregate normally. (*B*) Attachment of the centromeres of a given sister chromatid to opposite spindle poles. Resolution occurs through chromosome breakage. Filled circles, centromeres; thin lines, endogenous DNA; dashed lines, kinetochore microtubules; open circles, spindle pole bodies. The 10-kb lacO cassette is located nearly equidistant from the 2 centromeres on each sister chromatid.

Fig. 3. In vivo chromatin recoil. In part (*A*), the 10-kb lacO cassette of the recoiling molecule is visible (motion proceeds toward the pole in the lower left corner of the image), while the molecule is in the taut conformation. The free end of the molecule is approximately 2.6 μm from the spindle pole. (*B*) Brightfield image showing mother cell and bud. (*C*) Kymograh of the relaxation event (event shown in further detail in Fig. 4 where stem and flower conformation is more apparent).

Fig. 4. In vivo chromatin relaxation. (*A*) In vivo chromatin relaxation montage with fluorescent intensity mapped to color. The region of decreased intensity between the 1.5 and 1 μm length, and near the base of the molecule is the result of an image processing routine implemented to remove out of plane fluorescence caused by other (nonchromatin) structures. The unaltered image is shown in Fig. S5 and Movie S1. (*B*) Fluorescence intensity trace along the length of the retracting molecule for 3 frames of the relaxation event.

resulting from soluble protein and fluorescent artifacts in the surrounding environment may obscure the signal emitted from the GFP-tagged chromatin. This difficulty has motivated our development of an in vitro system to reproduce the in vivo conformations to determine the suitability of the taut and stem and flower models for the chromatin relaxation. We therefore developed an analogous in vitro assay that closely mimics the in vivo scenario, but in which we can control force, viscosity, and chain length (described in the *SI Text*). In this system, DNA concatamers stretched to over 10 μm long in a buffer of known viscosity were identified as possible targets for data collection. In most cases, photoscission, the light induced rupture of DNA, occurred less than 10 s after initial identification of the target molecule, allowing the relaxation event to be recorded (Fig. 5). For relaxation events taking place in low viscosity buffers (approximately 1 cP), we are unable to observe a fast relaxation regime where the fluorescent intensity of the retracting polymer is uniform. Instead, in our first images we see a bright spot at the retracting end of the polymer and a uniformly slow relaxation where the polymer length shrinks with time according to the expected stem and flower scaling exponent of 0.5 (see Fig. S1). Here, the extremely rapid initial portion of DNA relaxation takes place at a time scale that is shorter than our data acquisition rate, preventing the identification of the taut conformation. By increasing the solvent viscosity, we are able to slow down the initial portion of the relaxation to a point where it is possible to capture multiple images of the taut regime. Fig. S2 shows that the stem and flower analysis technique does 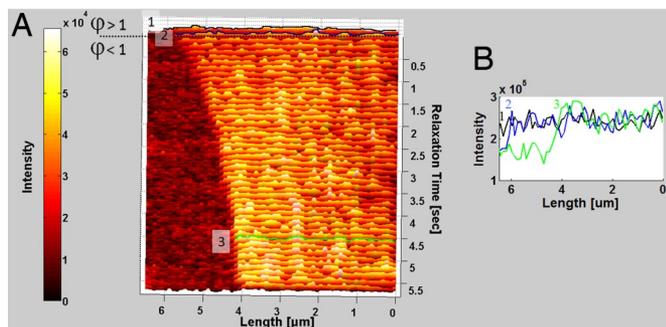not produce the expected scaling exponent when applied to relaxation data that contains both the taut and stem and flower conformations. As seen in Fig. 6, in a high viscosity environment, the DNA remains oriented along the force axis with the fluorescent intensity evenly distributed along the molecule for multiple frames. This is expected for the uniform relaxation

phenomena described by the taut relaxation. As the relaxation event proceeds, the fluorescent intensity at the retracting end eventually increases relative to the rest of the molecule (Fig. 6*C*), indicating the formation of the expected flower. Therefore, the intensity distributions along the DNA chain during relaxation identify the taut and the stem and flower relaxation regimes.

We can also identify these 2 regimes through an analysis of the relaxation dynamics. Applying the previously described universal scaling technique (10), we obtain the anticipated scaling exponent of approximately 0.5 (see Fig. 7*B* for examples) for the entire relaxation of the data obtained in low viscosity buffer. However, for the high viscosity data, the scaling analysis obtains the 0.5 exponent only by restricting the analysis to start at times after an initial induction period (see *SI Text*). This initial period shows a relaxation that deviates from the 0.5 exponent due to a faster process. We identify this as the taut relaxation, consistent with the uniform intensity of the images during this period. From the high viscosity multiregime relaxation data, we can extract the portion where the polymer is in the stem and flower conformation to determine the persistence length of the chain. Using the experimentally determined viscosity of 5.98 ± .02 P for the sucrose solution, the resulting experimentally determined persistence length of the retracting polymer is 40 nm. This persistence length, shorter than the typically observed value of approximately 50 nm (15), is most likely a due to the sucrose shielding the electrostatic repulsion of the DNA's negatively charged phosphate backbone.

For the taut regime of the DNA relaxation process, we determine a fast relaxation time constant to estimate the tension force on the chain. For the data shown in Fig. 6, the resulting time constant of $\tau = 4.8$ s, obtained by fitting the portion of the data in the taut conformation to an exponential decay function together with the previously determined chain length, allows us to determine a maximum tension force of 1.1 pN. These results indicate that it is reasonable to expect that a polymer released from tension retracting in a highly viscous fluid will take on both the taut (rod-like) and stem and flower conformations, validating our use of these techniques with our in vivo relaxation data to determine both the persistence length of the relaxing polymer and the tension force necessary to stretch the polymer before rupture.

Estimates of the Intranuclear Viscosity and Microtubule-Based Spindle Force. The in vivo data analysis requires knowledge of the viscosity of the nucleus or an estimate the persistence length of the retracting polymer. Due to the fact that published values for the intracellular viscosity as measured using the same probe size (100 nm) vary from approximately 10 P (16) to 520 P (17), we instead estimate the persistence length of the retracting polymer based on the polymer's initial length before rupture. For stretched DNA on a dicentric chromosome, the region of fluorescently labeled DNA/chromatin is 10 kb, which would result in an extended length of approximately 3.4 μm. For this data set, the structure stretched between the 2 poles has an

Fig. 5. DNA recoil in vitro. (*A*) DNA stretched between 2 attachment points ruptures due to photoscission. (*B*) Montage showing every other frame of a DNA relaxation event in a high viscosity buffer. The starting length of the molecule is approximately 6 μm, each new image is after the passage of 0.125 s. Data are shown in further detail in Fig. 6.

Fisher et al.

Fig. 6. In vitro dsDNA relaxation. (*A*) DNA relaxation event shown in Fig. 5 with image intensity mapped to color. Data collected at 16 fps. (*B*) Intensity plot for 3 frames of the DNA relaxation. In trace 1 (black), the entire molecule has an approximately constant intensity value which is lower that the value for trace 2 (blue). In trace 3 (green), the stem and flower conformation is apparent by the increased intensity value at the retracting end at approximately 4.0 μm. A movie of a similar relaxation event may be found in the SI (Movie S2).

are 2 requirements to observe entropic DNA relaxation in the taut conformation. They are (*i*) a uniform tension force that exceeds the linear entropic limit for the polymer and (*ii*) a sufficiently slow relaxation to allow for the collection of multiple images. With the force required to enter the nonlinear regime being relatively low, the "grab and pull" nature of microtubule-based spindle force easily meets the first criterion, while the intranuclear viscosity slows the relaxation to a rate that allows this conformation to be imaged. This high intranuclear viscosity is also apparent for the stem and flower portion of the chromosomal DNA relaxation. As seen in Fig. 6, the in vivo relaxation rate is significantly slower than the in vitro relaxation in an environment almost 600 times more viscous than water.

While the in vivo viscosity values obtained from our entropic relaxation experiments are quite high, and significantly higher than values measured using fluorescence recovery after photobleaching (FRAP) and fluorescence correlation spectroscopy (FCS) (19–21), these findings compare favorably with those determined using microbead rheology (16, 17) (10–2,200 P) and those calculated from the diffusion coefficients of Cajal bodies in the intranuclear region of HeLa cells (2.3–230 P) (20). This discrepancy, as pointed out by Tseng et al. (17), is a result of the different probe charges and sizes used in the experiments, with many FRAP and FCS experiments relying upon the diffusion of small proteins that measure the interstitial viscosity of the nucleus. The remaining techniques, including DNA relaxation described herein, measure properties at a length scale larger than the effective mesh size, resulting in motion that is constrained by the high concentration of proteins and larger molecules inside the nucleus, as well as interactions that are shape- (i.e., linear versus branched polymer diffusion) and charge-dependent. This dependence on charge was demonstrated by Lukacs et al. (19) using FRAP to measure diffusion coefficients of dextran and DNA molecules in the nucleus. They report nearly immobile DNA fragments as small as 21 bp, whereas dextran molecules up to 580 kDa diffuse at approximately one-fifth the rate at which they diffuse in water. Therefore, we believe our extremely high mesoscale viscosity measurement is relevant for the movement of larger bodies, on the length scale of nuclear organelles and perhaps whole chromatids, while the lower viscosity corresponds to that which is experienced by smaller proteins.

The force exerted by the microtubule-based spindle, estimated from the portion of the relaxation in the taut conformation, falls within the broad range of forces reported in the literature even though our technique and associated assumptions (most importantly the viscosity) differ greatly from what has been used in other approaches. Traditionally, this force has been determined using the simplified Stokes' equation $F = \gamma v$, where γ is the friction due to viscous resistance, and v is the velocity of the chromatid toward the pole. The coefficient of viscous resistance depends upon both the dimensions of the chromatid (*s*) and the
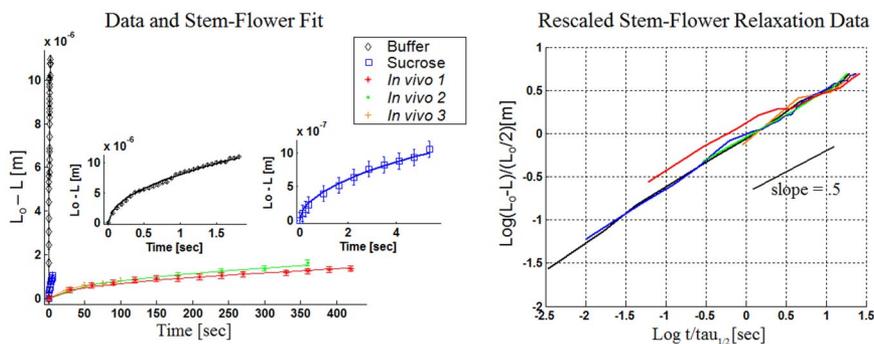
estimated prerupture length that corresponds to the completely extended length of this 10 kb, indicating that the DNA is not packaged as chromatin at the time of rupture. As a result, we have used the value of 50 nm for the persistence length of B-form DNA (18). With this assumption, the stem and flower model may be applied to the portion of the data with the appropriate fluorescent signature and the slower relaxation (example data set shown in Fig. 4 and labeled as In Vivo 1′ in Fig. 7), yielding an intracellular viscosity of 175 P. This viscosity is relatively large and will be discussed below. The fast relaxation time constant $\tau_1 = 167$ s, combined with the estimated persistence length and the previously determined viscosity, results in a tension force of 0.2 pN. The average intracellular viscosity we obtained by applying this analysis to the 3 in vivo events was 141 ± 29.2 P. This falls within the previously mentioned broad range of published values. The large standard deviation is due to a number of factors that may include different persistence lengths for the relaxing chromatin as well as heterogeneous viscosity regions inside the cell. For example, since the value that is input into the stem and flower model for the persistence length is inversely proportional to the output viscosity, a persistence length that is ±10% of our estimated value, possibly due to the interactions between the lacO-lacI-GFP system and the molecule, would alter the viscosity by ±10%.

Discussion

Chromosomal DNA behaves as an entropic spring in vivo, with very similar properties to those of naked DNA recoiling in a high viscosity environment. As seen in our in vitro experiments, there

Fig. 7. Stem and flower relaxation comparison. (*Left*) Relaxation data post taut conformation fit to the stem and flower model (Eq. **2**) for both in vitro and in vivo experiments. (*Right*) Universally scaled stem and flower data showing the expected scaling exponent of approximately 0.5. Systematic slight elevations from this exponent may be the result of Zimm-like hydrodynamic screening where by the solvent moves along with the retracting molecule (i.e., it is not free draining).

viscosity of the surrounding environment (η), yielding F = $\eta s v$. As a result, knowledge of the viscosity is critical for this type of analysis. In his seminal paper on forces applied to chromosomes, Nicklas estimated 1 P to be a plausible upper limit for the viscosity, which resulted in a calculated spindle force of approximately 0.1 pN (22). Using a similar technique but with the cytoplasmic viscosity measured using the Brownian displacements of particles located near the chromosomes, Alexander et al. (23) estimated the force to be 1–70 pN when using a viscosity of 2.82 P. While these estimated viscosities differ greatly from our measured value and that of other groups for the "mesoscale" viscosity, a critical observation from Nicklas (24) can help to explain the similarity between the forces estimated using a simplified version of Stokes' law and the force we estimate. Specifically, the fact that force as large as 100 pN applied in opposition of the spindle force, exerted during anaphase by a microneedle, does not decrease the velocity of the poleward movement. This means that the spindle's compliance (ability to maintain chromosome velocity under a range of loads) would most likely cause the chromatid to move at the same rate, regardless if the viscosity is 1 P as suggested by Nicklas, or 141 ± 29.2 P as reported here. As a result of the spindle's compliance, the simplified Stokes' method for estimating the spindle force does not accurately describe this system. Instead it may be better represented using Michaelis-Menten type kinetics, as suggested by Cytrynbaum (25), which is usually used to describe molecular motors.

As we discussed in the Introduction, both of the analysis techniques we have used are entropic in origin. An examination of the taut analysis parameter space (Fig. S3) shows that for a wide range of polymer persistence lengths and environmental viscosities, the force exerted by the microtubule-based spindle will be in the sub-pico-Newton range. As a result, errors in the estimated value for the persistence length and errors in the viscosity determined using the stem and flower model will not greatly affect the reported force.

At the time of release, the DNA/chromatin in the in vivo experiments is extended as if it has 0.2 pN of force applied to its end. To put our measured force into context, 0.2 pN converted to $k_b T$/nm units (1 $k_b T$/nm = 4.1 pN at 300 K) is approximately 0.05 $k_b T$/nm (0.2/4.1 = 0.05). As previously stated, we expect the DNA chain to be in the taut conformation when the theoretical tension blobs, or the length scale at which the conformation is randomized by 1 $k_b T$, have the same diameter as the chain's persistence length. Assuming the persistence length of the relaxing molecule to be 50 nm results in a work done per length of 0.02 $k_b T$/nm (1 $k_b T$/50 nm), putting the threshold to take on the taut conformation well below our measured value (0.05 spindle versus 0.02 thermal force). The next significant threshold would be that required to see nucleosome removal from the chromatin fiber. In vitro nucleosome disruption experiments performed in ATP-rich *Xenopus* extracts have shown that the application of approximately 2 pN of force can lead to nearly complete chromatin fiber disassembly (26). The resulting force per unit length of 0.49 $k_b T$/nm is above our observed value, indicating that our measured tension force at rupture was not large enough for nucleosome disruption. As previously stated, the fact that the chromatin was stretched out to the anticipated B-form DNA length indicates that nucleosome disruption had already taken place before the relaxation event. This indicates that either the force required for in vivo nucleosome disruption is an order of magnitude lower than what was observed in the in vitro *Xenopus* experiments or that the spindle force on the dicentric chromosome modulates with time. Without a doubt, the latter takes place on some time scale, since each disruption event corresponds to the release of the approximately 56 nm (165 bp) of DNA that is wrapped around the nucleosome. This increase in length will decrease the tension force until the slack is taken up. Additionally, the removal of nucleosomes will modify the persistence length of the molecule, making it similar to that of B-form DNA with negative supercoils, and thus alter the extension of the molecule for a given force. We are currently developing an experimental technique that will allow relaxation data to be collected from dicentric chromosomes at well-controlled time points during the force application in an effort to measure how the tension force on the chromatin fiber varies with time.

The relatively weak force in the microtubule-based spindle is consistent with previous in vivo results as well. Bouck and Bloom (27) reported an increase in spindle length (approximately 50%) upon a 50% reduction of nucleosomes. The increase in length can be attributed to the increased length of the pericentric chromatin. From the number of nucleosomes in the pericentric chromatin (approximately 42 nucs/strand), we estimate that there are 21 fewer nucleosomes upon histone reduction. The release of DNA from 21 nucleosomes yields (21 × 165 bp/nuc) approximately 3,500 bp DNA. The pericentric chromatin is organized as 32 parallel strands in series. The absolute increase in spindle length is 800 nm, thus each DNA strand stretches to approximately 34% its contour length (2 × 3,500 bp = 7kb; 7,000 × 0.3 nm/bp = 2,300 nm). The amount of force to stretch 1 naked DNA molecule to approximately 34% the contour length is less than 0.1 pN. Since the strands are in a series of 2 × 32 parallel clusters, we can estimate the total force from the worm-like chain model to be 1.6 pN.

We believe that our use of the taut conformation relaxation analysis previously described by Brochard-Wyart (11) is well motivated by the data obtained for both the in vitro and in vivo experiments. However, we acknowledge that there are other data analysis techniques that describe polymer relaxation in this regime that would result in alternative reported values for the force applied by the spindle apparatus. While our impetus was not to prove or disprove existing models, we believe that the experimental techniques developed herein can be used for such an undertaking. Specifically, it would be informative to test the predictions of the Brochard-Wyart model that omits polymer memory against those proposed by Hallatschek (28) that do not.

Conclusion

We have used a noninvasive genetic strategy to determine the biophysical properties of DNA in living cells. At the relatively high viscosities and applied cellular forces, relaxing DNA will take on the anticipated taut conformation which then gives way to the stem and flower conformation. These conformations have been verified using an in vitro system that enables relaxation dynamics to be investigated in solutions of known viscosity, allowing the experimentally determined persistence length to be compared with the anticipated value. In instances where the contour length and the persistence length of the relaxing molecule are known (or reasonably estimated), these 2 models may be used in combination to determine the viscosity of the surrounding environment, as well as the tension force applied before relaxation. The result of in vivo work is an estimation of the mesoscale viscosity inside the nucleus as well as an estimation of the force that was applied by the microtubule-based spindle apparatus to stretch chromatin. We believe that this data analysis technique offers advantages over existing methods because it is (*i*) noninvasive and (*ii*) the measured spindle force is for a relevant biological load, i.e., the chromatid.

Materials and Methods

Chromatin Relaxation In Vivo. A conditional dicentric chromosome has been constructed in budding yeast by means of site-directed integration of a second copy of centromere 3 (*CEN3*) at the *HIS4* locus (29). This extra copy of *CEN3* is regulated by the *GAL1* promoter (*GALCEN*), allowing cells to be propagated in the presence or absence of a functional dicentric chromosome. The dicentric

chromosome is functionally monocentric when cells are grown on galactose and functionally dicentric in the presence of glucose. If both centromeres on the dicentric chromosome attach to microtubules from the same spindle pole, chromosome segregation can occur without chromosome breakage (Fig. 2*A*). If centromeres from the same sister chromatid attach to microtubules from opposite poles, the chromosome stretches and breaks (Fig. 2*B*).

To visualize chromatin relaxation in live cells, a 10-kb lac operator repeat was integrated at *LEU2*, placing it nearly equidistant from both the endogenous *CEN3* and the *GALCEN3*. The marked chromosome was made visible by expression of lacI-GFP. This lacI-GFP/lacO marker system has been used previously to track individual chromosomes in living yeast cells and also changes in chromosome condensation within domains of mammalian chromosomes (30). Cells containing either a lacO-marked monocentric chromosome or a lacO-marked dicentric chromosome were imaged by time-lapse digital fluorescence microscopy. A lacO array located on a monocentric chromosome appeared as 1 spot that subsequently divided into 2 spots as the cells entered anaphase (14). In contrast, we observed the formation of a linear filament after activation of a lacO-marked dicentric chromosome in *sir2* mutant cells (14). In the majority of cells, stretched lacO filaments persisted for an average of approximately 30 min, followed by spindle collapse and the recoil of the chromatin filament to the neck of the budded cell (14).

Relaxation events are observed using a 1.4 NA 100× objective (Nikon) with images collected every 300 ms using Hammamatsu C2440 camera (Hamamatsu). Images are analyzed using the Image J measurement tool (National Institutes of Health) to determine the length of the retracting polymer. For the in vivo data analysis, the measurement error is ±130 nm.

DNA Relaxation In Vitro. In vitro samples were made by allowing concatamers of λ DNA to form via biotin/streptavadin and anti-Dig/Dig linkers. These long strands are attached to a coverslip surface with digoxigenin FAB fragments. The glass is initially stripped of organic compounds using an oxygen plasma, making it a high-energy negatively charged surface, then treated with APTES to modify the surface with amine groups that are coupled to the -COOH end of the FAB fragment during an EDAC reaction. The FAB-treated coverglass is soaked in BSA for 2 h to reduce nonspecific binding before addition of derivitized DNA. Dig/anti-Dig bonds between the molecule and the modified surface form DNA tethers at one end, while the remaining free end is stretched via thermal forces or flow during surface rinsing to binding sites on or near the surface. For high viscosity relaxation experiments, the viscosity of the surrounding fluid was elevated by the addition of sucrose, and the final viscosity of the fluid measured using a cone and plate viscometer (Ares G2; TA Instruments).

DNA stretched between 2 attachment points is cut using a photoscission process previously observed by Houseal and coworkers (31). Here, high-intensity light is absorbed by the DNA, causing the helix to rupture (Fig. S4). Rupture rates are controlled using an oxygen scavenging buffer and β-mercaptoethanol to prevent multiple breaks in 1 strand. DNA labeled with either Sytox Green or Sytox Orange is imaged using a 1.4 NA 100× oil immersion objective with a 1.5× magnification multiplier in place for the high-viscosity data collection, with images collected using a high-sensitivity camera (Cascade II; Photometrics) operating at 16 and 50 frames per second. Polymer length is then measured from these images using the Image J measurement tool, resulting in measurement errors of ±176 nm, with the 1.5× multiplier in place, and ±118 nm without.

1. Perkins TT, Quake SR, Smith DE, Chu S (1994) Relaxation of a single DNA molecule observed by optical microscopy. *Science* 264:822–826.
2. Wirtz D (1995) Direct measurement of the transport-properties of a single DNA molecule. *Phys Rev Lett* 75:2436–2439.
3. Perkins TT, Smith DE, Larson RG, Chu S (1995) Stretching of a single tethered polymer in a uniform-flow. *Science* 268:83–87.
4. Smith DE, Chu S (1998) Response of flexible polymers to a sudden elongational flow. *Science* 281:1335–1340.
5. Smith DE, Babcock HP, Chu S (1999) Single-polymer dynamics in steady shear flow. *Science* 283:1724–1727.
6. Doyle PS, Ladoux B, Viovy JL (2000) Dynamics of a tethered polymer in shear flow. *Phys Rev Lett* 84:4769–4772.
7. Mannion JT, Reccius CH, Cross JD, Craighead HG (2006) Conformational analysis of single DNA molecules undergoing entropically induced motion in nanochannels. *Biophys J* 90:4538–4545.
8. Perkins TT, Smith DE, Chu S (1997) Single polymer dynamics in an elongational flow. *Science* 276:2016–2021.
9. Brochard-Wyart F (1995) Polymer-chains under strong flows-stems and flowers. *Europhys Lett* 30:387–392.
10. Manneville S, Cluzel P, Viovy JL, Chatenay D, Caron F (1996) Evidence for the universal scaling behaviour of a freely relaxing DNA molecule. *Europhys Lett* 36:413–418.
11. Brochard-Wyart F, Buguin A, de Gennes PG (1999) Dynamics of taut DNA chains. *Europhys Lett* 47:171–174.
12. Kratky O, Porod G (1949) Röntgenuntersuchung aufgelöster Fadenmoleküle. *Recueil* 68:1106–1122.
13. Brochard F (1995) DNA-observing stems and flowers. *Physics World* 8:24–25.
14. Thrower DA, Bloom K (2001) Dicentric chromosome stretching during anaphase reveals roles of sir2/ku in chromatin compaction in budding yeast. *Mol Biol Cell* 12:2800–2812.
15. Baumann CG, Smith SB, Bloomfield VA, Bustamante C (1997) Ionic effects on the elasticity of single DNA molecules. *Proc Natl Acad Sci USA* 94:6185–6190.
16. Daniels BR, Masi BC, Wirtz D (2006) Probing single-cell micromechanics in vivo: The microrheology of *C. elegans* developing embryos. *Biophys J* 90:4712–4719.
17. Tseng Y, Lee JSH, Kole TP, Jiang I, Wirtz D (2004) Micro-organization and visco-elasticity of the interphase nucleus revealed by particle nanotracking. *J Cell Sci* 117:2159–2167.
18. Smith SB, Finzi L, Bustamante C (1992) Direct mechanical measurements of the elasticity of single DNA-molecules by using magnetic beads. *Science* 258:1122–1126.
19. Lukacs GL, Haggie P, Seksek O, Lechardeur D, Freedman N, Verkman AS (2000) Size-dependent DNA mobility in cytoplasm and nucleus. *J Bio Chem* 275:1625–1629.
20. Platani M, Goldberg I, Lamond AI, Swedlow JR (2002) Cajal body dynamics and association with chromatin are ATP-dependent. *Nat Neurosci* 4:502–508.
21. Seksek O, Biwersi J, Verkman AS (1997) Translational diffusion of macromolecule-sized solutes in cytoplasm and nucleus. *J Cell Biol* 138:131–142.
22. Nicklas RB (1988) The forces that move chromosomes in mitosis. *Annu Rev Biophys Biophys Chem* 17:431–449.
23. Alexander S, Rieder C (1991) Chromosome motion during attachment to the vertebrate spindle: Initial saltatory-like behavior of chromosomes and quantitative analysis of force production by nascent kinetochore fibers. *The J Cell Biol* 113:805–815.
24. Nicklas RB (1983) Measurements of the force produced by the mitotic spindle in anaphase. *J Cell Biol* 97:542–548.
25. Cytrynbaum EN, Sommi P, Brust-Mascher I, Scholey JM, Mogilner A (2005) Early spindle assembly in *Drosophila* embryos: Role of a force balance involving cytoskeletal dynamics and nuclear mechanics. *Mol Biol Cell* 16:4967–4981.
26. Yan J, et al. (2007) Micromanipulation studies of chromatin fibers in *Xenopus* egg extracts reveal ATP-dependent chromatin assembly dynamics. *Mol Biol Cell* 18:464–474.
27. Bouck DC, Bloom K (2007) Pericentric chromatin is an elastic component of the mitotic spindle. *Curr Biol* 17:741–748.
28. Hallatschek O, Frey E, Kroy K (2007) Tension dynamics in semiflexible polymers. II. Scaling solutions and applications. *Phys Rev E Stat Nonlin Soft Matter Phys* 75:031906.
29. Hill A, Bloom K (1989) Acquisition and processing of a conditional dicentric chromosome in *Saccharomyces cerevisiae*. *Mol Cell Endocrinol* 9:1368–1370.
30. Belmont AS, Straight AF (1998) In vivo visualization of chromosomes using lac operator-repressor binding. *Trends Cell Biol* 8:121–124.
31. Houseal TW, Bustamante C, Stump RF, Maestre MF (1989) Real-time imaging of single DNA-molecules with fluorescence microscopy. *Biophys J* 56:507–516.